Electronic Supplementary Material (ESI) for New Journal of Chemistry.

From Propargyl Alcohol-Water to the Propargyl Alcohol Dimer: Where does the Propargyl Alcohol-Methanol fit in?

Jyoti Saini* and K. S. Viswanathan

Department of Chemical Sciences, Indian Institute of Science Education and Research,

Mohali, Punjab 140306, India.

Supporting Information

Table S1. Uncorrected ΔE_{RAW}, zero-point energy corrected ΔE_{ZPC} and BSSE corrected ΔE_{BSSE} interaction energies (in kcal/mol) for different PA-MeOH hydrogen bonded complexes at M06-2X and ωB97X-D methods using aug-cc-pVDZ basis set.

	M06-2X/aug-cc-pVDZ			ωB97X-D/aug-cc-pVDZ		
	ΔE_{RAW}	ΔE_{ZPC}	ΔE_{BSSE}	ΔE_{RAW}	ΔE_{ZPC}	ΔE_{BSSE}
1	-9.0	-7.3	-8.4	-8.6	-6.8	-8.1
1A	-8.9	-7.3	-8.3	-8.6	-6.8	-8.0
1'	-7.2	-5.9	-6.7	-7.5	-6.0	-7.1
1'A	Not Optimized			-7.1	-5.7	-6.6
2	-6.4	-5.0	-5.8	-6.0	-4.6	-5.5
2'	-5.7	-4.4	-5.2	-5.5	-4.2	-5.2
2'A	-5.8	-4.6	-5.3	-5.4	-4.1	-5.0
3	-3.8[a]	-2.9[a]	-3.3[a]	Not Optimized		
4	-5.3	-4.1	-4.7	-4.8	-3.6	-4.3
4'	-4.2	-3.3	-3.7	-4.3	-3.1	-3.8
5	Not Optimized			Not Optimized		

[a] Opt=tight convergence criteria was relaxed for this PA-MeOH complex geometry

Table S2. Some of the important geometrical parameters for higher energy PA-MeOH complexes computed at MP2/aug-cc-pVDZ level. Bond distances are given in Å and angles in degrees.

	O···H	O-H···O	H···C_1	H···C_2	C-H···C_1	C-H···C_2	$C_2C_4O_7H_{14}$	$O_7H_8O_{13}H_{14}$	$O_7H_8O_{13}C_9$	$O_7H_{14}O_{13}C_9$
2	1.970	151.6	3.246	2.856	157.0	139.7	-97.2	-91.5	+133.8	+78.0
2'	1.918	159.5	-	-	-	-	+172.1	+51.8	+69.7	+139.9
2'A	1.948	152.0	-	-	-	-	-99.2	-153.0	-51.9	-68.7

3	O···H	≡C-H···O	H···C_1	H···C_2	C-H···C_1	C-H···C_2	$C_1H_3O_{13}H_{14}$	$C_1H_3O_{13}C_9$
	2.106	165.8	-	-	-	-	-150.9	-14.2

4	O_7···H_{11}	C_9H_{11}···O_7	H···C_1	H···C_2	O-H···C_1	O-H···C_2	$C_4H_6O_{13}H_{14}$	$O_{13}H_{14}C_1H_3$
	2.643	151.2	2.592	2.408	160.7	133.6	-28.8	+156.0
	O_{13}···H_6	C_4H_6···O_{13}						
	2.644	120.1						

4'	O···H	C-H···O	H···C_1	H···C_2	O-H···C_1	O-H···C_2	$C_4H_6O_{13}H_{14}$	$C_4H_6O_{13}C_9$	$O_{13}H_{14}C_1H_3$
	2.721	101.7	2.351	2.594	127.9	156.2	-46.6	+71.2	-172.5

5	O_7···H_{11}	C_9H_{11}···O_7	H···C_1	H···C_2	C-H···C_1	C-H···C_2	$C_4H_6O_{13}H_{14}$	$O_{13}H_{14}C_1H_3$
	2.806	113.8	3.253	2.867	141.8	122.2	-76.3	+157.2
	O_{13}···H_6	C_4H_6···O_{13}						
	2.347	144.3						

Table S3. Computed scaled vibrational features (in cm^{-1}) for the PA, MeOH and higher energy PA-MeOH hydrogen bonded complexes. Scaling factor for the O-H stretching region is 0.9548 and for the C-O stretching region is 0.9851. IR intensities (km/mole) have been indicated in brackets.

Computed scaled at MP2/aug-cc-pVDZ							
Monomers							
PA				**MeOH**			
3642.0 (38)				3667.3 (34)			O-H stretch
1040.8 (102)				1027.5 (112)			C-O stretch
PA-MeOH Complexes							
2	**2'**	**2'A**	**3**	**4**	**4'**	**5**	**Modes**
3637.6 (42) -4.4	3630.5 (43) -11.5	3637.8 (40) -4.2	3641.8 (35) -0.2s	3637.6 (39) -4.4	3642.7 (38) +0.7	3638.0 (36) -4.0	O-H st. in PA subunit
3572.0 (222) -95.3	3534.0 (466) -133.3	3563.1 (294) -104.2	3665.5 (43) -1.8	3620.0 (112) -47.3	3615.1 (161) -52.2	3661.2 (34) -6.1	O-H st. in MeOH subunit
1025.9 (79) -14.9	1021.7 (130) -19.1	1025.3 (95) -15.5	1037.1 (100) -3.7	1037.0 (141) -3.8	1039.7 (24) -1.1	1032.6 (112) -8.2	C-O st. in PA subunit
1038.8 (90) +11.3	1045.4 (90) +17.9	1041.6 (96) +14.1	1020.3 (104) -7.2	1023.8 (32) -3.7	1031.6 (234) +4.1	1015.1 (69) -12.4	C-O st. in MeOH subunit

Table S4. Experimental (in N_2) and computed scaled vibrational features for the PA, CD_3OD, CD_3OH and hydrogen bonded complexes **1** and **1A**, of PA-CD_3OD and PA-CD_3OH at the MP2/aug-cc-pVDZ level. Scaling factor for the O-H stretching region is 0.9548 and for O-D stretch is 0.9668. IR intensities (km/mole) have been indicated in brackets.

Experiment	Computed Scaled wavenumbers (cm^{-1})		Modes
Monomers			
	CD_3OD	CD_3OH	
3664.8		3667.1 (35)	O-H st.
2704.0	2704.1 (22)		O-D st.
PA subunit in PA-CD_3OD and PA-CD_3OH			
	Complex **1**	Complex **1A**	
3423.6, 3434.5	3429.9 (390)	3441.7 (370)	O-H st. for PA-CD_3OD
	3428.3 (355)	3440.5 (343)	O-H st. for PA-CD_3OH

Table S5. Experimental (in Ar matrix) and computed scaled vibrational features (in cm^{-1}) for the PA, MeOH and PA-MeOH hydrogen bonded complexes **1**, **1A**, **1'** and **1'A**. Scaling factor for the O-H stretching region is 0.9570 and for the C-O stretching region is 0.9872. IR intensities (km/mole) have been indicated in brackets.

Experimental		Computed scaled at MP2/aug-cc-pVDZ				
Monomers						
PA	**MeOH**	**PA**		**MeOH**		
3650.2	3667.0	3650.4		3675.7		O-H stretch
1042.9	1033.6	1042.9		1029.6		C-O stretch
Complexes						
PA	**MeOH**	Complex **1**	Complex **1A**	Complex **1'**	Complex **1'A**	**Modes**
3432.3		3434.0 (359)				O-H stretch in PA subunit
			3448.1 (342)			
				3446.7 (546)		
					3477.3 (446)	
	-	3584.4 (157)	3591.9 (128)	3657.0 (46)	3658.9 (48)	O-H stretch in MeOH subunit
1057.2		1055.7 (93)		1057.1 (99)		C-O stretch in PA subunit
			1059.2 (92)		1058.7 (86)	
1020.2		1016.9 (93)		1014.2 (91)	1018.6 (64)	C-O stretch in MeOH subunit
			1024.8 (92)			

Table S6. Electron density $\rho(\mathbf{r}_c)$, Laplacian $\nabla^2\rho(\mathbf{r}_c)$, local electronic kinetic energy density $G(\mathbf{r}_c)$, local electronic potential energy density $V(\mathbf{r}_c)$ and the hydrogen bonded energy E_{HB} values for the higher energy *gauche*PA-MeOH complexes, at the MP2/aug-cc-pVDZ level. The $\rho(\mathbf{r}_c)$, $\nabla^2\rho(\mathbf{r}_c)$, $G(\mathbf{r}_c)$, $V(\mathbf{r}_c)$ values given in atomic units and E_{HB} in kcal/mol. Values for *trans*PA-MeOH complex 6 has also been shown.

	Interaction	$\rho(\mathbf{r}_c)$	$\nabla^2\rho(\mathbf{r}_c)$	$G(\mathbf{r}_c)$	$V(\mathbf{r}_c)$	E_{HB}	total E_{HB}
*gauche*PA-MeOH Complexes							
complex **1'**	O-H···O	0.0324	0.1160	0.0288	-0.0287	-9.0	-9.9
	C-H···π	0.0067	0.0192	0.0039	-0.003	-0.9	
complex **1'A**	O-H···O	0.0282	0.1043	0.0249	-0.0238	-7.5	-8.5
	C-H···π	0.0071	0.0202	0.0041	-0.0032	-1.0	
	O-H···π	0.0119	0.0358	0.0077	-0.0066	-2.1	
complex **2**	O-H···O	0.0229	0.0836	0.0193	-0.0176	-5.5	-6.2
	C-H···π	0.0052	0.0165	0.0032	-0.0023	-0.7	
complex **2'**	O-H···O	0.0273	0.0959	0.0231	-0.0223	-7.0	-7.0
complex **2'A**	O-H···O	0.026	0.0836	0.0205	-0.0201	-6.3	-6.3
complex **3**	≡C-H···O	0.0173	0.0585	0.0131	-0.0116	-3.6	-3.6
complex **4**	C-H···O[a]	0.0083	0.0288	0.0058	-0.0044	-1.4	-4.8
	C-H···O[b]	0.0074	0.0243	0.0049	-0.0037	-1.1	
	O-H···π	0.0127	0.0393	0.0085	-0.0073	-2.3	
complex **4'**	C-H···O[a]	0.0066	0.0291	0.0055	-0.0038	-1.2	-3.6
	O-H···π	0.0132	0.0397	0.0087	-0.0076	-2.4	
complex **5**	C-H···O[a]	0.0131	0.0388	0.0086	-0.0074	-2.3	-3.9
	C-H···O[b]	0.0054	0.0211	0.004	-0.0027	-0.9	
	C-H···π	0.0054	0.0174	0.0034	-0.0024	-0.8	
	O-H···π	0.0119	0.0358	0.0077	-0.0066	-2.1	
*trans*PA-MeOH Complexes							
complex 6	O-H···O	0.0309	0.1131	0.0276	-0.027	-8.5	-8.5

Table S7. LMO-EDA results on the higher energy PA-MeOH complexes at MP2/aug-cc-pVDZ level. All energies provided in kcal/mol.

	E_{ES}	E_{EX}	E_{REP}	E_{POL}	E_{DISP}	E_{MP2}
1'	-12.6(33%)	-16.7(44%)	29.7	-4.5(12%)	-4.4(11%)	-8.5
1'A	-11.2(32%)	-15.3(44%)	27.1	-4.1(11%)	-4.6(13%)	-8.0
2	-8.6(31%)	-11.8(43%)	20.6	-2.7(10%)	-4.5(16%)	-6.9
2'	-9.2(35%)	-11.0(42%)	19.8	-2.9(11%)	-3.1(12%)	-6.4
2'A	-8.3(33%)	-10.6(42%)	18.9	-2.8(11%)	-3.6(14%)	-6.4
3	-5.4(34%)	-6.4(41%)	11.2	-1.9(12%)	-2.0(13%)	-4.4
4	-5.9(26%)	-10.0(44%)	17.0	-2.0(9%)	-4.7(21%)	-5.6
4'	-5.7(29%)	-8.8(44%)	15.2	-1.9(10%)	-3.4(17%)	-4.7
5	-4.1(24%)	-7.8(44%)	12.9	-1.5(8%)	-4.2(24%)	-4.6

Table S8. Correlation between the higher energy structures of PA-H_2O, PA-MeOH and PA-dimers, with their interaction energies, in kcal/mol, at the MP2/aug-cc-pVDZ level.

PA-H_2O	PA-MeOH	PA-dimers	
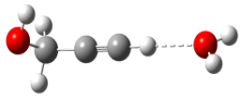 PAw3 (-3.7/-2.7/-2.7)	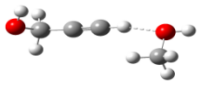 PAm**3** (-4.4/-3.6/-3.2)	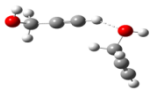 PAd9 (-4.6/-3.8/-3.2)	Not optimized
Precursor of PAm**5** (Not optimized)	 PAm**5** (-4.6/-3.8/-2.8)	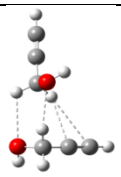 PAd8' (-5.4/-4.7/-3.2)	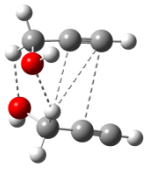 PAd8 (-5.6/-4.9/-3.3)
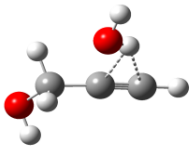 PAw4 (-4.1/-2.9/-2.8)	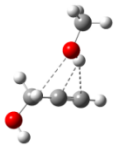 PAm**4'** (-4.6/-3.9/-3.1)	Not optimized	Not optimized
 Precursor of PAm**4** (Not optimized)	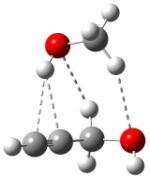 PAm**4** (-5.6/-4.6/-3.6)	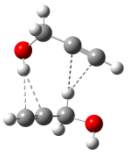 PAd6 (-7.1/-6.2/-4.6)	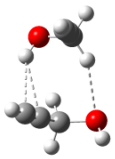 PAd7 (-6.9/-5.9/-4.3)
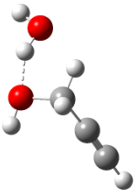 PAw2B (-5.8/-4.1/-4.6)	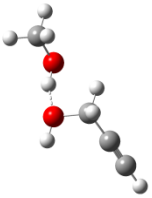 PAm**2'A** (-6.2/-5.1/-4.7)	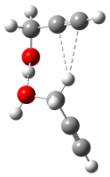 PAd2A (-8.3/-7.1/-6.1)	Not optimized
 PAw2 (-6.1/-4.2/-4.7)	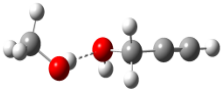 PAm**2'** (-6.3/-5.1/-4.8)	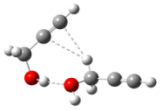 PAd2 (-8.4/-7.1/-6.1)	Not optimized
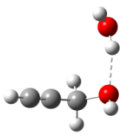 PAw2A (-5.8/-4.0/-4.6)	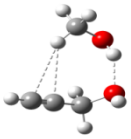 PAm**2** (-6.8/-5.6/-5.0)	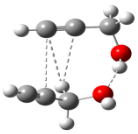 PAd4 (-8.6/-7.6/-6.3)	Not optimized

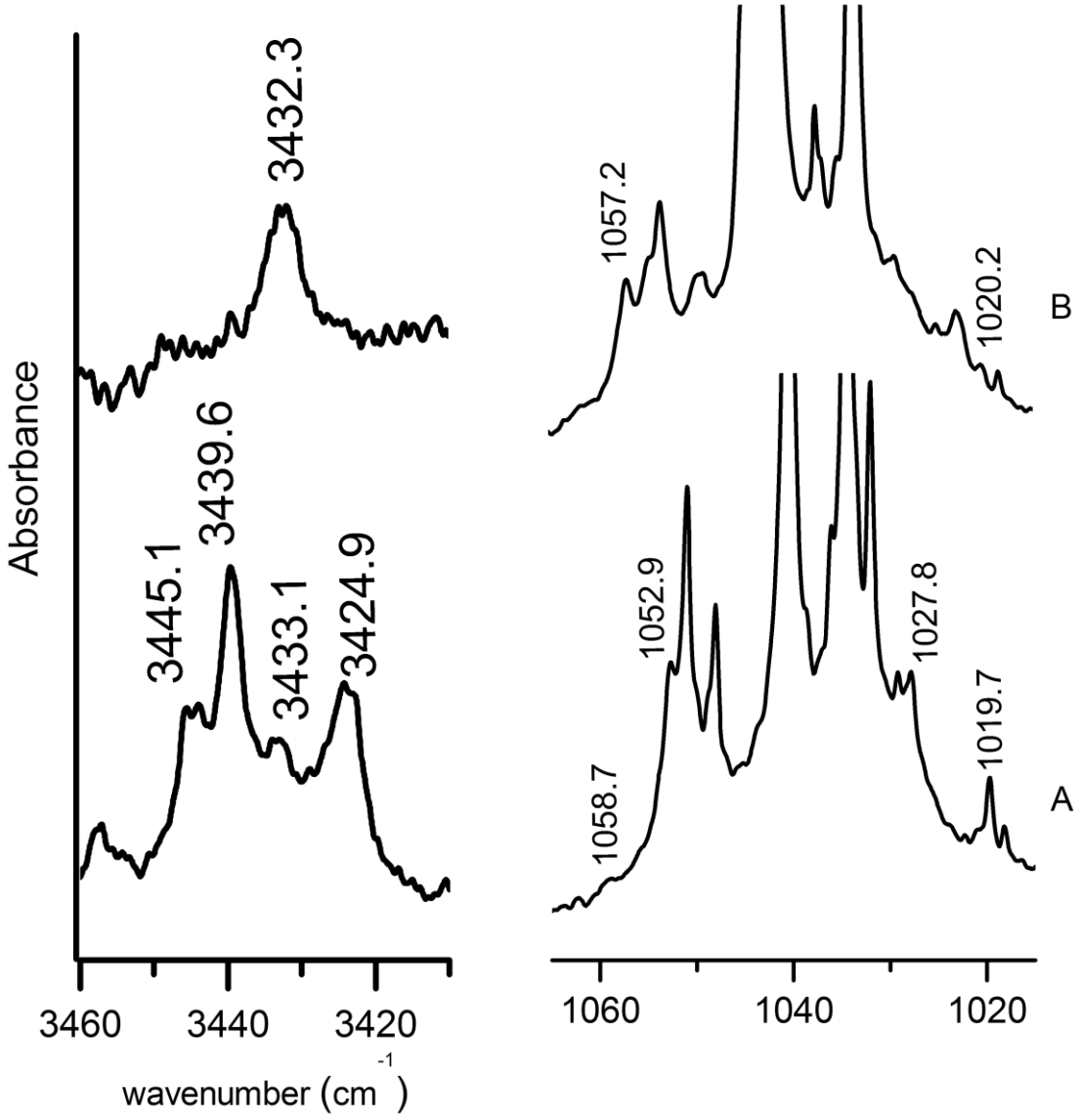

Fig. S1. Matrix Isolation Infrared spectra of PA codeposited with CH_3OH over the region 3460-3410 cm^{-1} and 1065-1015 cm^{-1}, with PA:CH_3OH in (A) N_2 matrix (3:3:1000) annealed at 27 K and (B) Ar matrix (10:5:1000) annealed at 32 K.

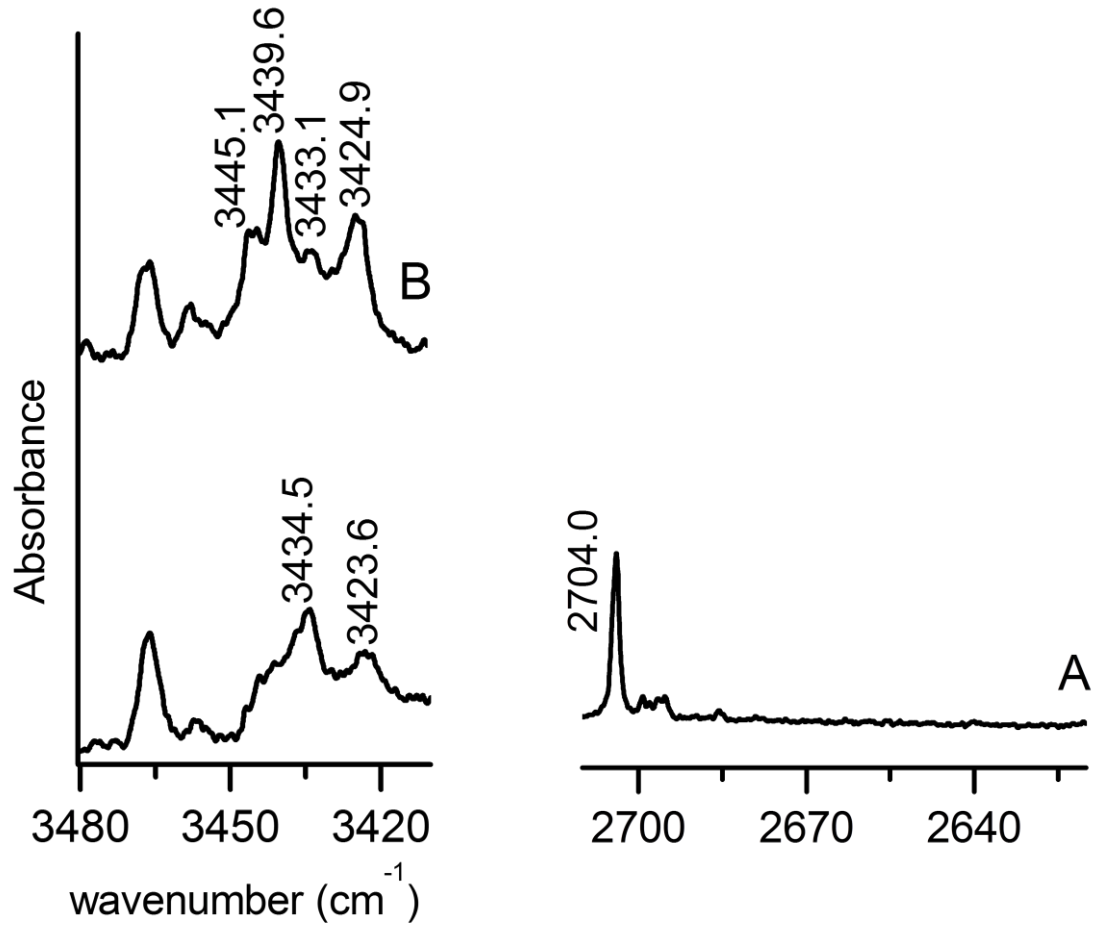

Fig. S2. Matrix Isolation Infrared spectra of PA:CD_3OD:N_2 (6:1:1000) is shown in Trace A, over the region 3480-3410 cm^{-1} (O-H stretch region of PA) and 2710-2620 cm^{-1} (O-D stretch region of CD_3OD. The spectra were recorded after annealing the matrix. For comparison, the spectra corresponding to the PA-CH_3OH system is also shown in Trace B for the region 3480-3410 cm^{-1}. (The O-D stretch in the PA-CD_3OD complex was computed to occur near 2645 cm^{-1} for complexes **1** and **1A**.)

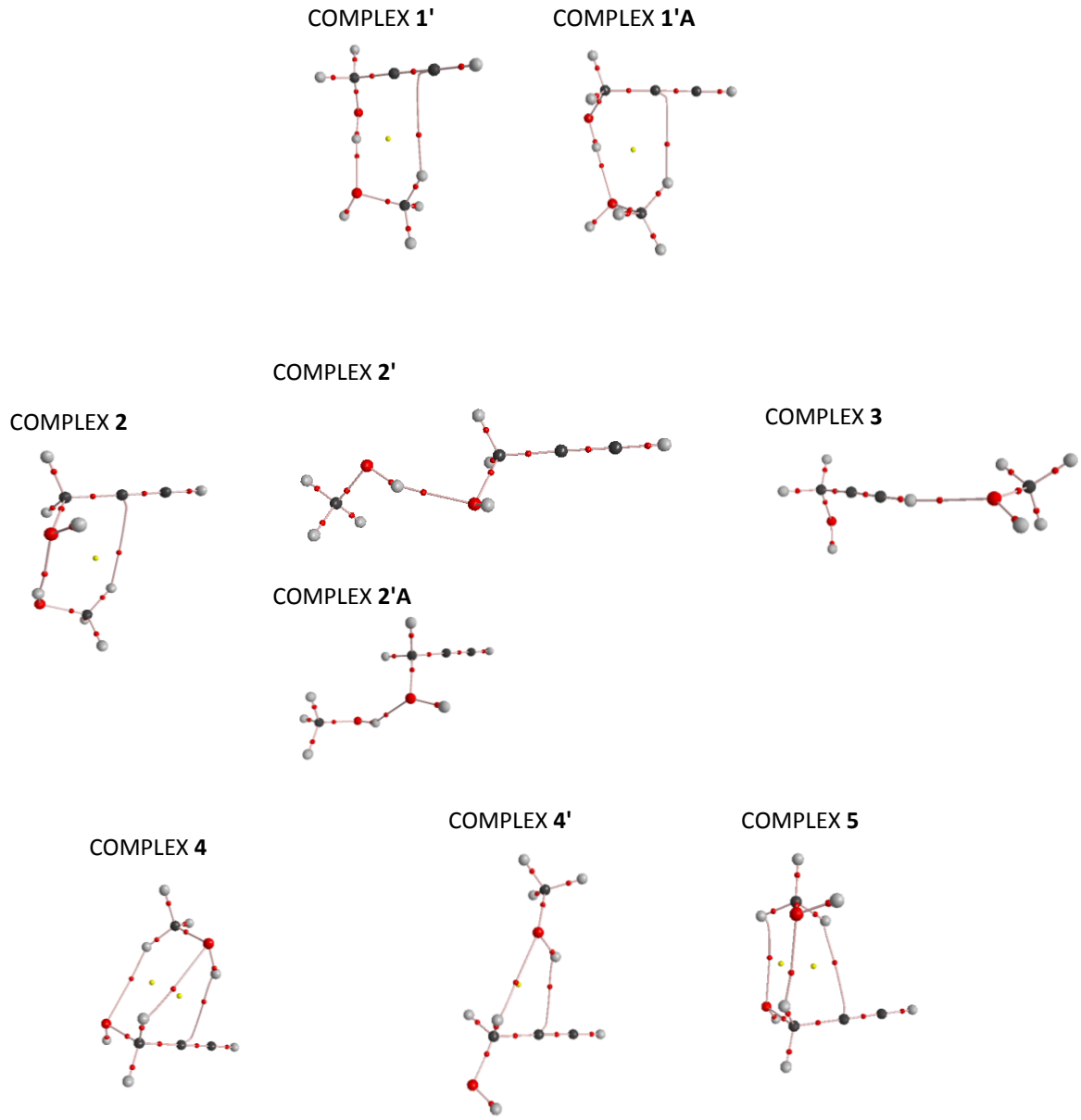

Fig. S3. AIM analysis for higher energy PA-MeOH complexes at MP2/aug-cc-pVDZ level showing the bond and ring critical points.